Linear sinusoidal phase-shifting method resistant to non-sinusoidal phase error

Haihua Cui (崔海华)*, Wenhe Liao (廖文和), Ning Dai (戴 宁), and Xiaosheng Cheng (程筱胜)

Jiangsu Key Laboratory of Digital Medical Equipment Technology, Nanjing University of Aeronautic and Astronautic, Nanjing 210016, China

**Corresponding author: cuihh@nuaa.edu.cn*

Received June 29, 2011; accepted September 5, 2011; posted online November 7, 2011

Non-sinusoidal phase error is common in structured light three-dimensional (3D) shape measurement system, thus we perform theoretical and experimental analyses of such error. The number of non-sinusoidal waveform errors in a 2π phase period is the same as the number of steps of the phase-shifting algorithm; no errors occur within the one-phase period. Based on our findings, a new structured light method, the linear sinusoidal phase-shifting method (LSPS), that is resistant to non-sinusoidal phase error is proposed. Experiments show that the non-sinusoidal waveform error is reduced to an almost negligible level (0.001 rad) using the proposed LSPS.

OCIS codes: 120.0120, 120.2650, 100.0100, 150.0150.
doi: 10.3788/COL201210.031201.

Optical non-contact three-dimensional (3D) shape measurement techniques have been developed to obtain 3D contours. With the recent advancement in digital display technology, 3D shape measurement based on digital projection units has been rapidly expanding[1−2]. However, the challenge remains to be in area of developing a system with an off-the-shelf projector, such as liquid crystal display (LCD) and digital mirror device (DMD), for high-quality 3D shape measurement. One of the major issues is the nonlinear response of the projection engines of projectors[1−10].

Projector gamma calibration is usually needed to perform high-quality 3D shape measurement using a digital fringe projection and phase-shifting method[2−10]. This is because the commonly used commercial video projector is a nonlinear device purposely designed to compensate for human vision[7]. A variety of techniques have been developed for nonlinear phase errors[2−12]. These include the two-step triangular-pattern phase-shifting algorithm and the error compensation method[5−6], which can reduce periodic measurement errors due to gamma nonlinearity as well as projector and camera defocus. In this letter, the detailed mathematical model for sinusoidal phase shifting was developed to predict the effects of non-unitary gamma on phase-measuring profilometry[3]. Zhang *et al.* developed a compensation method that needs to calibrate an error look-up table (LUT) and is based on the assumption of periodic phase error[9−10]. In general, the abovementioned methods need an additional compensatory step to reduce phase error. A new method with defocusing binary structured patterns can be used to eliminate nonlinear gamma[7]; however, controlling the proper defocusing degree to achieve high accuracy is difficult using this method[8]. Guo *et al.* proposed a gamma correction method using a simple one-parameter gamma function technique by statistically analyzing the fringe images[11]. These techniques significantly reduce the phase error caused by nonlinear gamma. Nevertheless, these compensation methods still have residual error value that cannot be ignored in accurate measurement. In addition, the actual gamma of the projector is very complicated and is not the only factor that causes non-sinusoidal waveforms. Our experiments show that the nonlinear gamma of the projector changes over pixels, and must be compensated one by one. All these problems hinder its applications, especially for precision measurement. Hence, a technique that is resistant to non-sinusoidal waveforms would be a significant development in 3D shape measurement.

In this letter, we present the linear sinusoidal phase-shifting method (LSPS), a novel coding method that combines the advantages of nonlinear waveform error resistance and the high resolution attained by the sinusoidal phase-shifting methods. Compared with the traditional phase-shifting method, the proposed method is far less sensitive to the projector nonlinear gamma. The idea originated from the following observations. Firstly, in a 2π phase period, the number of non-sinusoidal waveforms is the same as the number of the phase steps. Secondly, a few zero-error points occur in the 2π phase period. Finally, although the non-sinusoidal waveforms have periodicity, the distances between each cycle and the error amplitude are different. The last observation indicates that it is difficult to completely eliminate the phase error using the passively compensated algorithms[8−10], which are based on the same periodicity assumption. The first two observations imply that the error can be completely eliminated if the distance between each cycle is reduced to zero, and if the zero phase error pixels are selected. If this hypothesis is true, then a novel and robust phase coding method can be developed without nonlinear projector gamma calibration. Experiments are presented to verify the performance of the proposed technique.

Sinusoidal phase-shifting methods are widely used in optical metrology because of their measurement accuracy. In this letter, a four-step phase-shifting algorithm, which requires four phase-shifted images, is used. The intensities of the four images with a phase shift of $\pi/2$ are

$$I_j^{\mathrm{p}}(x,y) = I'(x,y) + I''(x,y)\cos[\varphi(x,y) + j \times \pi/2], \quad j = 0,\ 1,\ 2,\ 3. \tag{1}$$

where $I_j^{\rm p}(x,y)$ is the intensity value of pixel (x,y) in the jth fringe image, $I'(x,y)$ is the average intensity, $I''(x,y)$ is the intensity modulation, and $\varphi(x,y)$ is the phase to be datermined. Upon solving these four equations, the following phase can be obtained as

$$\varphi(x,y) = \arctan[(I_1 - I_3)/(I_0 - I_2)]. \tag{2}$$

Equation (2) provides the wrapped phase with 2π discontinuities. A spatial phase-unwrapping algorithm can be applied to obtain the continuous phase[13], which can be used to retrieve 3D coordinates[14].

Phase errors were analyzed in one period using the temporal-phase (TP) method, which is not necessary in measurement, in order to study their characteristics. Firstly, the computer-generated ideal sinusoidal patterns were sent to a projector. The fringe image was then moved, leaving one pixel in each projection plane. After T times of shifting (T is the number of points sampled), the intensities of the T grating images are obtained as

$$I_i^{\rm p}(x,y) = I^{\rm p}(x+i,y),\ i = 1,\ 2,\ \cdots,\ T. \tag{3}$$

These sinusoidal patterns were captured by a camera with an intensity of $I_i^{\rm c}(x,y)$:

$$I_i^{\rm c}(x,y) = I'(x,y) + I''(x,y)\cos[\varphi_i^{\rm c}(x,y)],\quad i = 1,\ 2,\ \cdots,\ T. \tag{4}$$

Based on the four-step phase-shifting algorithm, the phase $\varphi_i^{\rm c}(x,y)$ of each pixel can be calculated as follows. $\varphi_i^{\rm c}(x,y)$ is the modulo 2π phase at each pixel with value ranging from 0 to 2π:

$$\varphi_i^{\rm c}(x,y) = \arctan\left[\frac{I^{\rm c}_{i+1\times\frac{T}{4}}(x,y) - I^{\rm c}_{i+3\times\frac{T}{4}}(x,y)}{I^{\rm c}_{i+0\times\frac{T}{4}}(x,y) - I^{\rm c}_{i+2\times\frac{T}{4}}(x,y)}\right],\quad i = 1,\ 2,\ \cdots,\ T. \tag{5}$$

If $(i + j\times\frac{T}{4}) > T$, $i = 1,\ 2,\ \cdots,\ T$, $j = 0,\ 1,\ \cdots,\ 3$, then $(i + j\times\frac{T}{4}) = (i + j\times\frac{T}{4}) - T$.

Based on the TP method, one circle phase $\varphi_i^{\rm c}(x,y)$ of each pixel was calculated by Eq. (5), and the phase error $\Delta\varphi_i^{\rm c}(x,y)$, which is the difference between the current and the ideal phases, was obtained. The ideal phase is a linear one ranging from 0 to 2π; thus, the slope of the line ranging from 0 to 2π is the phase error $\Delta\varphi_i^{\rm c}(x,y) = \varphi_i^{\rm c}(x,y) - kx$, where $k = 2\pi/T$. The red lines in Fig. 1 denote the phase errors of the 500th row on 20 different pixels of the image. The phase errors with fringe pitches of 20 and 8 have root-mean-square (RMS) values of 0.076 and 0.021 radians, respectively.

Figure 1 clearly shows the following. Firstly, four sinusoidal phase error cycles exist in each wrapped phase (0–2π), and the number of phase error cycles is the same as the number of steps of the phase-shifting algorithm. Secondly, nonlinear errors in a wrapped phase (0–2π) have zero error points at $i\times T/8$ ($i = 1,\ 2,\ \cdots,\ 8$). Thirdly, the magnitudes and spaces of the phase errors decrease continuously with the decrease in fringe pitch. Lastly, the projector nonlinear gamma changes over pixels, resulting in a different phase error that causes the non-sinusoidal waveform to be incompletely compensated by positively

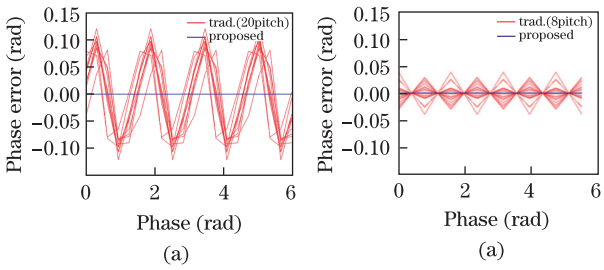

Fig. 1. (Color online) Comparison between (a) the traditional and (b) the proposed method. Phase error (red lines) for traditional fringe patterns and phase error (blue line) with the proposed fringe pattern.

compensated algorithms[8−10].

The above observations can be explained in theory. The first phenomenon is caused by the principle of the four-step phase-shifting algorithm. The phase values of each pixel are determined by a four-pixel gray value with an interval $T/4$, as shown in Eq. (5). This means that one circle phase is divided into four equal parts: $(0,\ T/4]$, $(T/4,\ 2T/4]$, $(2T/4,\ 3T/4]$, and $(3T/4,\ T]$. Each part is computed using the same gray value with interval $T/4$, as shown in Eq. (5). Thus, there are four phase error circles in one wrapped phase. The phase is computed with the arctangent trigonometric function shown in Eq. (5). The arctangent function has convergent properties at $\pm\pi/2$ positions, where the computed phase value $\varphi_i^{\rm c}(x,y)$ slightly changes even if there are dramatic changes in the domain, as $\left[\frac{I^{\rm c}_{i+1\times\frac{T}{4}}(x,y) - I^{\rm c}_{i+3\times\frac{T}{4}}(x,y)}{I^{\rm c}_{i+0\times\frac{T}{4}}(x,y) - I^{\rm c}_{i+2\times\frac{T}{4}}(x,y)}\right]$. Hence, this convergence characteristic significantly reduces the nonlinear response of the projector gamma at points $i\times T/8$ ($i = 1,\ 2,\ \cdots,\ 8$).

The first three points mentioned above show that if the number of pixels in $T/4$ is reduced to 1, that is a wrapped phase (0–2π) period of four pixels $T = 4$, then the phase error spaces are reduced to 1, which is the only four-phase error value in a wrapped phase. In addition, if zero error points are also selected to compute the phase, then the phase error is theoretically and completely eliminated. Figure 2 shows the cross-sections and the gray image of the four patterns. Their intensities can be written as

$$I^{\rm p}(x,y) = I'(x,y) + I''(x,y)\cos[(x\times 2\pi)/4 + j\times\pi/2],\quad j = 0,\ 1,\ 2,\ 3. \tag{6}$$

Equation (6) indicates that only the intensity values of 0, 255/2, and 255 are used for their novelty and simple, structured light pattern. The phase was computed using a traditional four-step phase-shifting algorithm – the LSPS algorithm. The phase error with our fringe pattern, computed using the TP method, is 0; this is represented as the blue lines in Fig. 1.

The proposed fringe pattern has a triangular pattern; however, the proposed method differs from the triangular phase-shifting method[4−6], which uses triangular patterns coded with gray levels for the projection. Calculating the captured triangular patterns obtains a triangular intensity ratio distribution. Removing the triangular shape of the intensity ratio through each full pattern

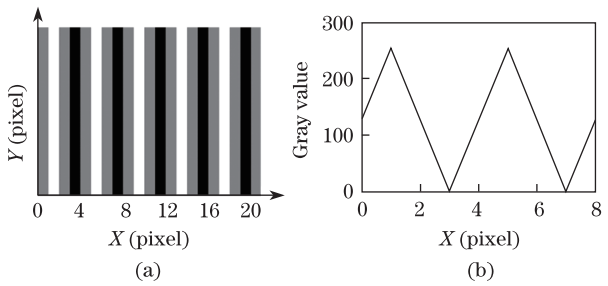

Fig. 2. Proposed linear sinusoidal phase-shifted fringe pattern. (a) Gray image of the proposed pattern; (b) cross-section of the proposed fringe pattern.

pitch generates a wrapped intensity ratio distribution. These methods have a simple computation for the intensity ratio and rapid calculation speed. However, they are highly sensitive to noise, nonlinearities, and projector and camera defocus[6]. Our proposed method and the triangular pattern method differ in three ways. Firstly, our linear sinusoidal curve is consistent with the sine function, whereas the triangular method is not. Secondly, phase calculation is different, with our method being based on the calculation of an arctangent function of the phase, whereas the triangular method computes the intensity ratio to obtain the phase. Thirdly, our method is immune to the non-sinusoidal phase error, whereas the measurement accuracy of the triangular method is limited by the gamma nonlinearity[6].

Two traditional sinusoidal fringes are tested to compare the performance of the proposed approach and the traditional phase-shifting fringe methods. The phase error is calculated using the TP method, as previously specified. The phase error corresponding to the real wrapped phase value is plotted in Fig. 1. The phase error with traditional sinusoidal fringe phase-shifting method is very clear, as shown by the red lines in Fig. 1, although the four cycles of phase errors at each point are the same. However, the phase error between the two points is different; the phase error with the proposed LSPS algorithm is zero and is completely eliminated, as shown by the blue lines in Fig. 1.

In practice, the calculated phase value is affected by the nonlinear gamma curve, object independent irradiance function, gray interpolation, and image noise, among others[2]. This causes the different values for the magnitudes and spaces of the four periodic phase errors that were calculated using the spatial phase method (Fig. 3). To further verify the LSPS method, a 3D shape measurement system was built comprising a DMD projector (NP50+, NEC, Japan) and a USB CCD camera (OK_AM1310, Jiahengzhongzi, China) with a Computar 1614-MP lens F/1.4 with f of 16 mm. The system measure area is about 100×100 (mm) and the camera resolution is $1\,280 \times 1\,024$ pixels. The digital video projector shows the proposed four phase-shifted linear sinusoidal images with a phase shift of $\delta_1 = 0°$, $\delta_2 = 90°$, $\delta_3 = 180°$, and $\delta_4 = 270°$, and the CCD camera captures the reflected fringe images with a white flat board. In this verification, traditional sinusoidal fringes with 20 and 8 pitches are used as examples to create the phase error. Figures 3(a) and (b) show the plot of the 500th row with respect to the wrapped phase. The red lines in Figs. 3(a) and (b) illustrate the phase error with traditional sinusoidal fringes, while the blue lines show the phase error with the proposed method. Figures. 3(c)–(e) show the 3D reconstruction results with the traditional and the proposed methods. The figure shows a part of the white flat board, which is about 80×80 (mm). The phase errors with fringe pitches of 20 and 8 have RMS values of approximately 0.078 and 0.022 radians, respectively. In comparison, the phase error with the proposed fringe pattern is reduced to an RMS value of 0.001 radians. The phase error is almost eliminated or completely minimized, showing that the proposed linear sinusoidal gray patterns play a significant role in weakening the nonlinearity of the projector gamma.

In addition, a plaster tooth model was measured, and no filter algorithm was used to smoothen the 3D geometry. The part of the plaster tooth model with a volume of about $40 \times 25 \times 10$ (mm) is measured and reconstructed. Figure 4 shows the reconstructed 3D model with the traditional and the LSPS methods. Figure 4(a) shows the projected fringe image, while Figs. 4(b) and (c) present the results of the reconstruction with traditional sinusoidal fringe pitches of 20 and 8. Figure 4(d) shows the result of the reconstruction with the LSPS method. The reconstructed 3D geometric surface with the proposed method is smoother and has better visual

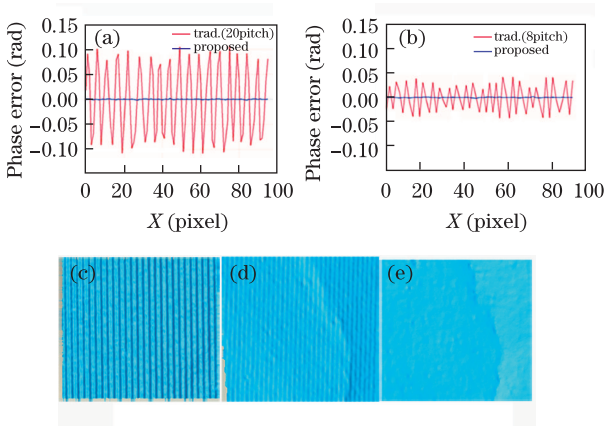

Fig. 3. (Color online) 3D measurement result of the flat board with the traditional and the proposed methods. (a)–(b) 500th row of the phase error with traditional sinusoidal fringes and the proposed fringe; (c)–(d) 3D reconstruction with traditional sinusoidal fringe pitches of 20 and 8; (e) 3D reconstruction with the proposed method.

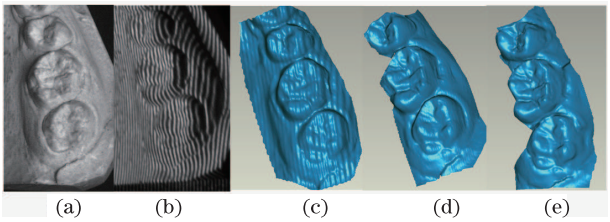

Fig. 4. 3D measurement result of the complex plaster tooth model with the traditional and the proposed methods; (a)–(b) source image and phase-shifted fringe image for the plaster model; (c)–(d) 3D geometry with traditional sinusoidal fringe pitches of 20 and 8; (e) 3D geometry with the proposed method.

effects, confirming that the proposed LSPS method can successfully eliminate or minimize non-sinusoidal waveforms and significantly improve measurement accuracy.

As stated above, the number of phase error cycles in the wrapped phase (0–2π) is the same as the number of the steps of the phase-shifting algorithm. This indicates that the pitch of one phase error cycle is equal to $1/n$ of the fringe pattern (n is the step of the phase-shifting algorithm). The number of phase errors changed to 1 when the pitch of one phase error cycle is decreased to 1; zero error pixels are then selected for computation, and the phase errors are eliminated. Thus, the proposed method is not only suitable for four patterns, but also for different numbers (the number n) of the pattern in principle.

The proposed phase-shifting fringe pattern has four pixels in one period. The projected fringe patterns seem to be very thin when measuring large objects. Thus, it is important to know how to capture striped images without being affected by the defocus and pixel splitting of the camera, and by the resolution difference between the camera and the projector. We used laser to certify the captured patterns in focus and found that the two other factors mainly cause the pixel gray interpolation. An additional laser line and the camera center line form a triangle structure, which can be used to detect the appropriate measurement distance.

The proposed phase-shifting method has the following advantages. Firstly, the LSPS algorithm is far less sensitive to the nonlinear gamma of the projector because of its novel principle, and the convergent properties of the arctangent trigonometric function are used. Secondly, in theory, the error caused by the nonlinear gamma of a digital video projector can be almost completely eliminated while still maintaining the advantage of a phase-shifting-based approach, which makes it an accurate tool for 3D shape measurement system. Thirdly, the proposed LSPS algorithm is simple, using linear sinusoidal patterns with only three kinds of gray, which have clear differences in tonal value.

In conclusion, we present a novel and robust structured light, linear sinusoidal phase-shifting method for 3D shape measurement. Compared with traditional sinusoidal phase-shifting methods, the proposed method has the advantages of non-sinusoidal waveform error resistance since it eliminates the errors from the principle of generation, instead of calibrating the nonlinear response of the projector. In general, the proposed algorithm solves the issues encountered in 3D profile measurement system using a digital projector.

This work was supported in part by the National "863" Program of China (No. 2009BAI81B02) and the Doctoral Foundation of Ministry of Education (No. 20070287055).

References

1. S. Gorthi and P. Rastogi, Opt. Laser. Eng. **48,** 133 (2010).
2. G. H. Notni and G. Notni, Proc. SPIE **5144,** 372 (2003).
3. K. Liu, Y. Wang, D. L. Lau, Q. Hao, and L. G. Hassebrook, J. Opt. Soc. Am. A **27,** 553 (2010).
4. B. A. Rajoub, D. R. Burton, and M. J. Lalor, J. Opt. A **7,** S368 (2005).
5. P. Jia, J. Kofman, and C. English, Opt. Eng. **46,** 043601 (2007).
6. P. Jia, J. Kofman, and C. English, Opt. Laser Eng. **46,** 311 (2008).
7. S. Lei and S. Zhang, Opt. Lett. **34,** 3080 (2009).
8. S. Lei and S. Zhang, Opt. Laser. Eng. **48,** 561 (2010).
9. S. Zhang and P. S. Huang, Opt. Eng. **46,** 601 (2007).
10. S. Zhang and S.-T. Yau, Appl. Opt. **46,** 36 (2007).
11. H. Guo, H. He, and M. Chen, Appl. Opt. **43,** 2906 (2004).
12. B. Pan, Q. Kemao, L. Huang, and A. Asundi, Opt. Lett. **34,** 416 (2009).
13. H. Cui, W. Liao, X. Cheng, N. Dai, and T. Yuan, Chin. Opt. Lett. **8,** 33 (2010).
14. B. Liu, P. Wang, Y. Zeng, and C. Sun, Chin. Opt. Lett. **8,** 666 (2010).